



# Ion beam analysis of deuterium-implanted $\text{Al}_2\text{O}_3$ and tungsten

R.G. Macaulay-Newcombe<sup>\*</sup>, D.A. Thompson

*Department of Engineering Physics, McMaster University, Hamilton, Ont. L8S 4L7, Canada*

## Abstract

Single crystal tungsten and  $\text{Al}_2\text{O}_3$  (sapphire), and polycrystalline WESGO-995  $\text{Al}_2\text{O}_3$  samples were implanted with 20–30 keV deuterium at 300–500 K. The deuterium distributions were determined using  $^3\text{He-D}$  nuclear reaction analysis, at 300–800 K. The results indicated that considerable diffusion occurred both during the implantations and during the subsequent analysis. Modelling the data indicates effective (radiation-enhanced) diffusivities as high as  $10^{-16}$   $\text{m}^2/\text{s}$  in  $\text{Al}_2\text{O}_3$ , compared to a thermal diffusivity  $\sim 10^{-41}$   $\text{m}^2/\text{s}$  at 300 K [J.D. Fowler, D. Chandra, T.S. Elliman, A.W. Payne, K. Verghese, *J. Am. Ceram. Soc.* 60 (1977) 155.]. The modelling also suggests that most of the implanted deuterium was released at the surface, although a significant fraction diffuses to depths greater than the expected ion range. In tungsten, implanted deuterium is trapped at defects that appear to be mobile at 300 K, enabling the deuterium distribution to extend much deeper than the ion range. At higher temperatures the trap energy appears to increase with time. Modelling the data indicates little deuterium release through the front surface, i.e. most diffused deeper into the bulk of the sample. © 1998 Elsevier Science B.V. All rights reserved.

## 1. Introduction

Tungsten and  $\text{Al}_2\text{O}_3$  represent two classes of candidate plasma-facing materials: metals and ceramics. Tungsten is being considered as a high-flux wall armour material, whereas  $\text{Al}_2\text{O}_3$  is an RF window material and a typical insulator. Before these materials can be approved for use in ITER, it is important to establish how tritium will be retained and released during and after plasma bombardment. This will affect tritium inventories and component properties. This paper compares the behaviour of single crystals to polycrystalline  $\text{Al}_2\text{O}_3$ , and metal to ceramic, under deuterium and helium ion irradiation at temperatures from 300 to 800 K.

## 2. Experimental

The samples were: (a) high-purity single crystal tungsten from Johnson-Matthey; (b) single crystal, RF-

grade  $\text{Al}_2\text{O}_3$  (sapphire) from Crystal Systems; and (c) polycrystalline  $\text{Al}_2\text{O}_3$  (WESGO-995) from Dr. R. Stoller at ORNL. All samples were polished to a mirror finish before implantation.

The samples were implanted with 60 keV  $\text{D}_2^+$  or  $\text{D}_3^+$  ions (20–30 keV per deuteron) at fluxes of  $2\text{--}15 \times 10^{16}$   $\text{D}/\text{m}^2 \text{ s}$ , to fluences of  $2\text{--}15 \times 10^{20}$   $\text{D}/\text{m}^2$ . These fluxes resulted in ionization and elastic defect creation rates close to those predicted for ITER [1], i.e.  $\sim 10^4$  Gy/s of ionizing radiation, and  $\sim 10^{-6}$  dpa/s of elastic (collisional) radiation. The relatively high ion energies resulted in implanted deuterium depth distributions large enough to be resolved by NRA, and hence compared to TRIM-96 (SRIM) predictions [2].

The analysis ions were 0.8–1.5 MeV  $^3\text{He}^+$ , at fluxes of  $1\text{--}5 \times 10^{17}$  ions/ $\text{m}^2 \text{ s}$ , to total accumulated fluences of  $10^{19}\text{--}10^{21}$  ions/ $\text{m}^2$ . The ionization and elastic defect creation rates from the analysis ions were similar to those of the implant ions. Aluminum foils, ranging in thickness from 2.9–6.6  $\mu\text{m}$ , were used to filter out the scattered  $^3\text{He}$  ions from the 2–5 MeV  $^4\text{He}$  reaction product [3]. During analysis the sample would be tilted at 60–75°, with the detector subtending a solid angle of 9 mStr at 30–60° to the incident ion direction.

<sup>\*</sup> Corresponding author. Fax: +1-905 527 8409; e-mail: macnew@mcmaster.ca.

### 3. Results

#### 3.1. Single crystal $Al_2O_3$ (sapphire)

Fig. 1 shows deuterium depth profiles determined from NRA of sapphire implanted at 300 K with 60 keV  $D_3^+$  ions, to a fluence of  $1.4 \times 10^{21}$  D/m<sup>2</sup>. The integrated yield up to a depth of 620 nm was  $4.9 \times 10^{20}$  D/m<sup>2</sup>, which is  $\approx 36\%$  of the estimated implant fluence. This implies that most of the deuterium incident on the sample was desorbed during the implantation. Also shown is the ion range profile obtained from TRIM-96 [2] (with arbitrary amplitude). The measured depth profile extends about 100 nm deeper than predicted by TRIM, suggesting considerable diffusion during the implantation. Repeated analyses on the same spot resulted in no change in the deuterium profile.

After heating the implanted sample to 800 K, 9% of the deuterium was desorbed. As can be seen in Fig. 1, deuterium was lost from the near-surface region, but there was no change in the profile at depths  $>300$  nm. Again, there was no change in the deuterium profile due to the analysis ions.

Fig. 2 compares deuterium profiles following 300 and 500 K implants at the same fluence, followed by NRA at 300 K. For the 500 K implant, the retention was only  $\approx 20\%$ . The shapes of the deuterium profiles suggest that the extra loss is due to faster desorption during the 500 K implant.

In contrast to the behaviour of the 300 K implant, there was no further loss of deuterium after heating to 800 K, nor during NRA at 800 K over a period of 30 min.

#### 3.2. Polycrystalline $Al_2O_3$ (WESGO-995)

Fig. 3 shows deuterium depth profiles from NRA of WESGO-995 after implanting  $10^{21}$  D/m<sup>2</sup> 60 keV  $D_2^+$  ions

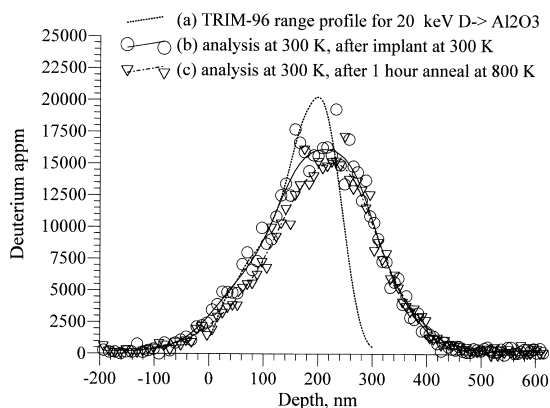


Fig. 1. Depth profiles of deuterium in sapphire after 300 K implant. Determined from NRA using 0.9 MeV  $^3He$  and 2.9  $\mu m$  Al foil.

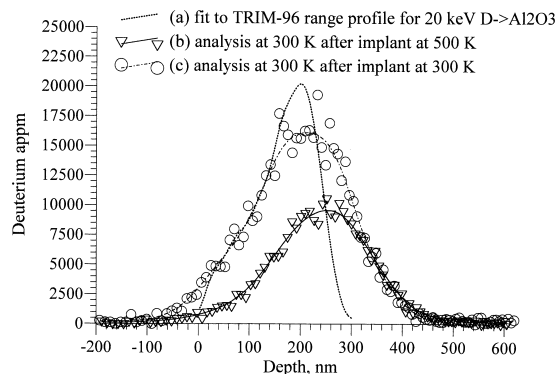


Fig. 2. Depth profiles of deuterium in sapphire after 500 K implant. Determined from NRA using 1.1 MeV  $^3He$  and 2.9  $\mu m$  Al foil.

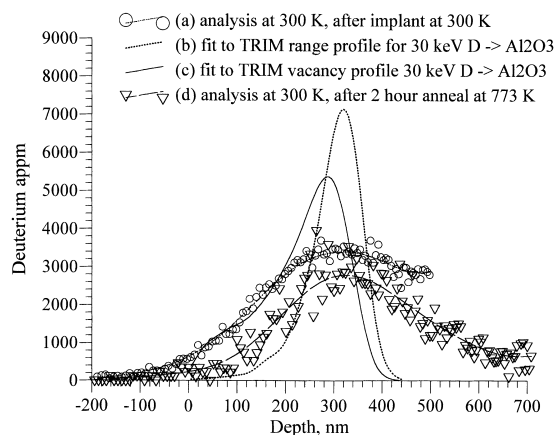


Fig. 3. Depth profiles of deuterium in WESGO-995 after 300 K implant. Determined from NRA using 0.95–1.1 MeV  $^3He$  and 6.4  $\mu m$  Al foil.

at 300 K. The TRIM-96 range and vacancy profiles are also shown (arbitrary amplitudes). Note that the measured deuterium profile extends below 500 nm, i.e. well beyond the predicted range. The fraction of deuterium retained is  $\approx 19\%$  (up to a depth of 500 nm), compared to 36% for sapphire.

The analysis ions had no effect on the deuterium distribution at 300 and 500 K. In contrast, when the sample was heated to 773 K and analysed repeatedly on the same spot, the deuterium profile decreased in amplitude, while maintaining the same shape. Fig. 3(d) shows the depth profile after a flux of  $10^{21}/m^2$  analysis ions over a period of 2 h at 773 K: the integrated yield of deuterium up to a depth of 500 nm dropped by 32%.

Fig. 4 shows the deuterium depth profile in WESGO-995 implanted with  $1.5 \times 10^{21}$  D/m<sup>2</sup> as 60 keV  $D_3^+$  ions

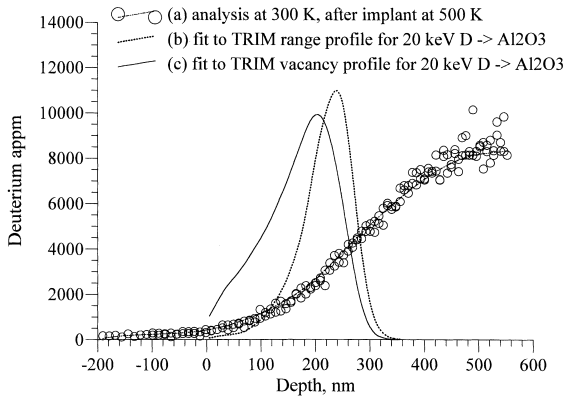


Fig. 4. Depth profiles of deuterium in WESGO-995 after 500 K implant. Determined from NRA using 1.1 MeV  $^3\text{He}$  and 6.4  $\mu\text{m}$  Al foil.

at 500 K. Note that the deuterium profile extends well beyond the TRIM range profile, peaking at 550 nm or deeper. The fractional retention is  $>23\%$  of the implanted fluence, higher than observed after the 300 K implant. Clearly, more deuterium diffused into the sample and less was lost through the surface during the implantation. Analysis at 300–800 K had no effect on the deuterium distribution.

3.3. Single crystal tungsten

Single crystal W samples were implanted both at normal incidence and at  $75^\circ$  tilt. Fig. 5 shows deuterium depth profiles from NRA at 300 K, after implantation at 300 K with 60 keV  $\text{D}_3^+$  ions at a sample tilt of  $75^\circ$  and a fluence of  $2.3 \times 10^{20}$   $\text{D}/\text{m}^2$ . NRA was performed at

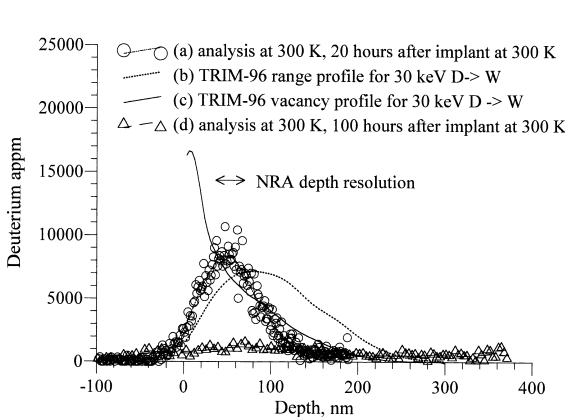


Fig. 5. Depth profiles of deuterium in single crystal tungsten after 300 K implant. Determined from NRA using 0.95–1.1 MeV  $^3\text{He}$  and 6.4  $\mu\text{m}$  Al foil.

various intervals, 20–100 h after the implant. After correcting for the deuterium ion reflection coefficient of  $\approx 30\%$ , the measured retention 20 h after the implant was  $>30\%$  of the net fluence. TRIM-96 [1] calculations of the ion range and vacancy profiles for the above implant conditions are shown for comparison. The depth resolution of the NRA was  $\approx 35$  nm, and the uncertainty in the location of the surface (due to detection geometry) was  $\approx 25$  nm.

Fig. 5(d) shows that 100 h after the implant, the deuterium had diffused well into the sample, and the retention (to a depth of 380 nm) was less than 14%. The distribution is nearly flat, and shows no indication of tailing off below 380 nm. Again, the analysis ions did not appear to affect the deuterium distribution.

Fig. 6 shows depth profiles of deuterium in single crystal tungsten after implantation at normal incidence, at 300 K, with 60 keV  $\text{D}_3^+$  ions to a fluence of  $1.7 \times 10^{21}$   $\text{D}/\text{m}^2$ . After accounting for the 12% reflection coefficient, the retention is  $\approx 30\%$  of the estimated net fluence, as was the case for the previous, much lower fluence implant. This is a lower limit to the retention fraction, since the profile in Fig. 6(a) appears to extend below the depth probed by NRA, 500 nm in this case. As before, the analysis ions did not appear to affect the deuterium profile. However, analysis 70 h after the implant showed no change in the deuterium profile, in contrast to the losses seen for the lower fluence, shallower implantation discussed above.

After heating the sample to 500 K the deuterium yield over the first 500 nm decreased to 21% of the net implant fluence. Multiple analyses over a space of 3 h at 500 K resulted in a further drop to 15%.

After cooling the sample to 300 K, there was a further small decrease (to 14%) in the amount of deuterium up to 500 nm depth, over the course of multiple NRA

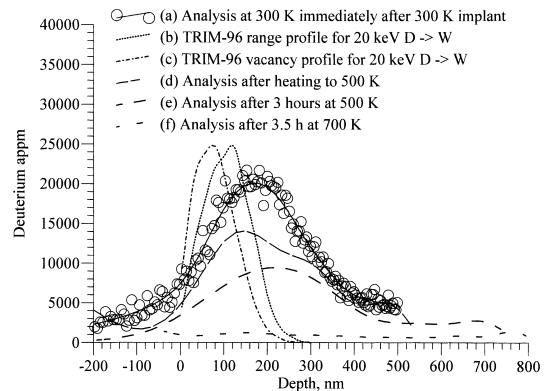


Fig. 6. Depth profiles of deuterium in single crystal tungsten after 300 K implant. Determined from NRA using 1.2–1.5 MeV  $^3\text{He}$  and 6.4  $\mu\text{m}$  Al foil. The lines are arbitrary smoothed fits to the data points (shown only in (a)).

analyses. The deuterium profile from 500–740 nm depth did not change during analysis when the NRA conditions were altered to probe more deeply.

Analysis after heating to 700 K revealed more loss of deuterium over the first 500 nm from the surface, to 9%; by the final analysis, after 3.5 h at 700 K, the peak yield had dropped to 2% of the net implant.

## 4. Calculations and discussion

### 4.1. Single crystal $Al_2O_3$ (sapphire)

The sapphire data has been studied using the diffusion calculation program TMAP-4 [4]. A radiation-enhanced diffusivity,  $D_{RE}$ , of up to  $10^{-16}$  m<sup>2</sup>/s is required to match the observed deuterium profile after implanting deuterium at 300 K. This is  $\gg 10^{-45}$  m<sup>2</sup>/s, the thermal diffusivity extrapolated from Fowler et al. [5] to 300 K. Furthermore, it was necessary to assume an enhanced diffusivity well beyond the ion range, in order to match the observed deuterium distributions.

The TMAP-4 calculations indicated the presence of traps of energy 0.7 eV, in concentrations of  $\approx 2$  at.%. This trap energy is consistent with the results of Myers et al. [6,7] in aluminium, where it was concluded that deuterium was trapped in small voids with an effective binding energy of 0.71 eV, attributed to the energy of formation of the  $D_2$  molecule. The calculations also indicated a surface recombination coefficient  $\approx 5 \times 10^{-36}$  m<sup>4</sup>/s. Using the Baskes model for recombination [8], a surface sticking coefficient of 0.001 (typical for ceramics) and the solubility for tritium in sapphire from Alexander et al. [9], the radiation-enhanced diffusivity becomes  $D_{RE} \approx 10^5$  m<sup>2</sup>/s  $\exp(-1.25 \text{ eV}/kT)$ , which produces  $D_{RE} = 10^{-16}$  m<sup>2</sup>/s at 300 K. In comparison, Fowler et al. [5] reported a thermal diffusivity of  $3.3 \times 10^{-4}$  m<sup>2</sup>/s  $\exp(-2.48 \text{ eV}/kT)$ . This suggests that: (a) the activation energy for diffusion was lowered from 2.48 to 1.25 eV, perhaps by ionization effects of the deuterium ions or by radiation damage induced strain; and (b) the pre-exponential ( $D_0$ ) was increased by a factor of  $3 \times 10^8$ , probably because of the much higher than equilibrium vacancy concentration. Since the enhanced diffusion appears to operate at depths greater than the ion range, these vacancies must be diffusing into the sample.

The slow diffusion and desorption of deuterium at 800 K suggests that the traps evolved as the temperature was raised, with the trap energy increasing to about 2 eV; otherwise, thermal diffusion would have resulted in profile broadening and surface desorption of deuterium.

Preliminary calculations for the 500 K implant suggest a similar  $D_{RE}$ , but with traps of  $>2$  eV to account for the lack of diffusion or desorption at 800 K.

### 4.2. Polycrystalline $Al_2O_3$ (WESGO-995)

Modelling of the WESGO-995 implant at 300 K yielded similar results to those for sapphire at 300 K, except that  $D_{RE} \approx 4 \times 10^{-16}$  m<sup>2</sup>/s during the implant. The desorption observed during the anneal at 773 K could be due to de-trapping induced by the analysis ions, or thermal de-trapping. The observation that the deuterium profile did not broaden during the anneal, but simply decreased in amplitude, suggests a relatively low concentration of empty traps, so that re-trapping is negligible.

Preliminary calculations for the 500 K implant suggest that  $D_{RE} \approx 10^{-15}$  m<sup>2</sup>/s, and the trap energies were  $>0.7$  eV.

### 4.3. Single crystal tungsten

TMAP-4 [4] calculations are in progress for the deuterium implantation, diffusion and desorption processes in tungsten. Input values being used are: the deuterium diffusivity in tungsten from [10]; the surface sticking coefficient, estimated as 0.25 (a typical value for a fairly clean metal surface); and a recombination coefficient at 300 K of  $10^{-37}$  m<sup>4</sup>/s, estimated with the Baskes model [8].

The thermal diffusivity predicted by extrapolating the results of Frauenfelder [10] to 300 K is  $D \approx 10^{-13}$  m<sup>2</sup>/s. Since this is much larger than the radiation-enhanced diffusivities estimated for  $Al_2O_3$  in Sections 4.1 and 4.2, it is not surprising that there is no radiation-enhanced diffusion effect observed for deuterium-implanted tungsten. In fact, the calculations indicate that traps are required to prevent the deuterium from diffusing into the bulk of the sample. To duplicate the deuterium profile and desorption during and after the first implant (see Fig. 5), two sets of traps are required: one with an energy of 0.74 eV, and a concentration  $\approx 0.8$  at.% from the surface to a depth of 60 nm, decreasing with increasing depth; the other with an energy of 1.2 eV, and a concentration of 0.18 at.% from the surface to 60 nm depth, also decreasing with increasing depth. This compares well with the results of Garcia-Rosales et al. [11], who obtained trap energies of 0.85 and 1.4 eV for tungsten implanted with 100 eV deuterium.

For the second implant, shown in Fig. 6, the fluence was much higher ( $1.5 \times 10^{21}$  D/m<sup>2</sup> versus the earlier  $1.6 \times 10^{20}$  D/m<sup>2</sup>). However, the deuterium retention was 30% of the net implant fluence in both cases. Initial TMAP-4 calculations indicate trap concentrations roughly double those in the previous implant, and extending deeper into the sample. The deeper profile is attributed to deuterium and defect diffusion from the implant zone. This is in agreement with the modelling of Garcia-Rosales et al. [11], which suggested that the implanted deuterium would be trapped at depths well beyond the implant zone.

## 5. Conclusions

Both  $\text{Al}_2\text{O}_3$  and W retain deuterium at concentrations up to several atomic per cent after ion implantation, at depths well beyond the implant zone. TMAP-4 [4] calculations suggest that this retention is due to trapping. After the implant, the rate of deuterium release from sapphire (single crystal  $\text{Al}_2\text{O}_3$ ) is very low, even at 800 K. The rate is higher from WESGO-995 (polycrystalline  $\text{Al}_2\text{O}_3$ ), and higher again from single crystal tungsten. The calculations are complicated by apparent changes in the nature of the traps with rising temperature.

Tritium diffusion at 300 K in  $\text{Al}_2\text{O}_3$  was not expected to be a problem for ITER. However, under neutron and tritium bombardment, radiation-enhancement of the diffusivity could result in tritium diffusing hundreds of micrometers into the bulk over the lifetime of ITER, resulting in significant tritium inventories.

For tungsten, with its high tritium diffusivity, permeation could be a serious problem, although it should be delayed somewhat by trapping at defects. The tritium inventory could reach as much as  $6.3 \text{ g/m}^2$  in 2 mm thick W first wall armour, given 1 at.% traps and low temperatures. Garcia-Rosales et al. [11] observed that deuterium implanted into tungsten at 100 eV was largely desorbed after heating to 650 K, and suggested that this might apply to ITER divertor armour made of tungsten. Even with radiation damage traps, such as those produced by neutrons (or 20 keV deuterium ions), the desorption results shown in Figs. 5 and 6 support this conclusion.

## Acknowledgements

The financial and technical support of the Canadian Fusion Fuels Technology Project (CFFTP) is gratefully acknowledged. Thanks are also due to Paul Gierszewski of CFFTP, and Glen Longhurst of INEL, for valuable discussions.

## References

- [1] S.J. Zinkle, *Plasma Devices Oper.* 3 (1994) 139.
- [2] J.F. Ziegler, J.P. Biersack, U. Littmark, SRIM (TRIM-96), similar to TRIM as described in *The Stopping Powers and Ranges of Ions in Solids*, Pergamon, New York, 1985.
- [3] R.G. Macaulay-Newcombe, M. Riehm, D.A. Thompson, W.W. Smeltzer, A. Abramov, *Radiat. Eff. Defects Solids* 117 (1991) 285.
- [4] J.L. Jones, B.J. Merrill, Tritium Migration Analysis Program, version 4, developed at INEL, manual by G.R. Longhurst et al., EGG-FSP-10315, 1992.
- [5] J.D. Fowler, D. Chandra, T.S. Elliman, A.W. Payne, K. Verhese, *J. Am. Ceram. Soc.* 60 (1977) 155.
- [6] S.M. Myers et al., *J. Nucl. Mater* 165 (1989) 9.
- [7] S.M. Myers, D.M. Follstaedt, *J. Appl. Phys.* 63 (1988) 1942.
- [8] M.I. Baskes, *J. Nucl. Mater.* 92 (1980) 318.
- [9] C. Alexander et al., Tritium Diffusion in Non-Metallic Solids of Interest for Fusion Reactors, DOE/ET/52022-5, 1979.
- [10] R. Frauenfelder, *J. Vac. Sci. Technol.* 6 (1969) 388.
- [11] C. Garcia-Rosales, P. Franzen, H. Plank, J. Roth, E. Gauthier, *J. Nucl. Mater.* 233–237 (1996) 803.